A BASIC STUDY ON EFFICIENCY IN JAPANESE AIRSPACE

Kota Kageyama* , **Yoshihiro Miyatsu***
***Electronic Navigation Research Institute**
{kage; miyatsu}@enri.go.jp;

Abstract

The efficiency in Japanese airspace is assessed to identify the airborne phase that requires intensive improvement. In this study, the efficiency is measured based on fuel-burn. Since it is considerably difficult to obtaining actual detailed data, the fuel-burn is estimated from the trajectories. For the estimation, the BADA (Base of Aircraft Data) table is used.

First, actual fuel-burn data and the estimation results are compared to validate the fuel-burn estimation model. Then, applying the estimation model to actual trajectory, fuel-burn is examined. Based on the estimation results, fuel-burn is compared among airborne phases.

1 Introduction

To accommodate the increase in air traffic demand, ATM has significantly improved its performance in the last few decades. However, since a higher quality of ATM service is required, further ATM performance improvement programs are being implemented.[1], [2]. To improve ATM performance in an effective manner, identification of bottlenecks is indispensable. Implementing intensive improvement of the bottlenecks, ATM performance should be enhanced. To identify the bottlenecks, ATM performance assessment is required.

Since ATM has, by definition, multiple objectives to accomplish, its performance must be assessed through multiple viewpoints. ICAO (International Civil Aviation Organization) has defined Key Performance areas comprised of 11

areas[3]. 'Efficiency', which is one of the KPI for ATM operation performance, is focused on in this paper.

Among the indexes, efficiency is measured based on excess fuel-burn. In European airspace, it was assessed that potential efficiency resided mainly in a horizontal en-route flight path[4]. Since airspace is being managed differently in each region, the aspect of the efficiency could be different in each airspace. Thus, the efficiency in Japanese airspace should be assessed.

This paper is comprised of two parts. Since there is considerable difficulty in obtaining actual data, the fuel-burn needs to be estimated. Therefore, the estimation model based on the BADA table is built for this study. Comparing with a small set of the actual fuel-burn data, the estimation results are validated.

Then, the estimation model is applied to actual trajectories on a Japanese representative route and excess fuel-burn is estimated. Based on the estimation results, efficiencies are compared among airborne phases.

2 The Fuel-burn Estimation

2.1 The Estimation Model

The estimation model was built based on the BADA 3.8 table. BADA is a collection of ASCII files which includes performance summary tables. In the table, climb, cruise and descent fuel-burn per unit-time at each flight level are defined for a wide variety of aircraft types[5].

Comparing current altitude with the last altitude, the model determined flight profile (climb,

Table 1 The Number of Flight Samples

Type	Sample #
B738	5
B763	16
B772	32

cruise and descent). Then, for the combination of current altitude and flight profile, the model extracted fuel-burn from the BADA table for each time-period. Accumulating the extracted value, fuel-burn for the entire flight was computed.

2.2 Validation of the Estimation Results

For the validation of the model, small sets of actual fuel-burn and trajectory data were obtained. The obtained samples covered three types of aircraft; Boing 737-800 (B738), Boeing 767-300 (B763) and Boeing 777-200 (B772). Table 1 shows the number of the data set for each aircraft type.

To measure the estimation error, the fuel-burn error ΔE_i for aircraft i is defined as follows;

$$\Delta E_i = (E_i - A_i)/A_i \tag{1}$$

where E_i is the estimated fuel-burn and A_i is the actual fuel-burn.

Fig. 1 shows the box-plots of the ΔE for each aircraft type. In this figure, the lower hinge represents the value of the first quartile ($Q1$) whereas the upper hinge represents the value of the third quartile ($Q3$). The upper whisker represents the highest value within the range of $Q3 + 1.5 \times (Q3 - Q1)$, whereas the lower whisker represents the lowest value within the range of $Q1 - 1.5 \times (Q3 - Q1)$. From the figure, it was observed that the ΔE for B763 demonstrated a wider spread, which implied that the estimation for B763 was less accurate than the others.

On the other hand, the ΔE for the other aircraft type demonstrated a small convergence. For instance, the hinges for B772 ranged from 0.2 %
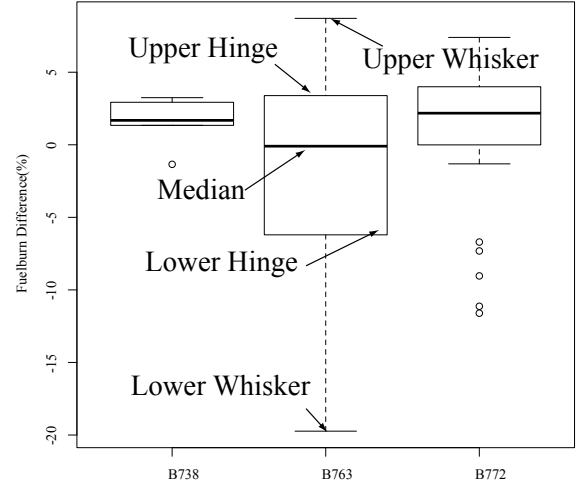
Fig. 1 The Box-plots of the ΔE_i
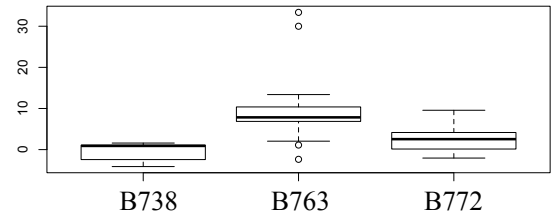
Fig. 2 The Box-plots of the ΔE_i^b
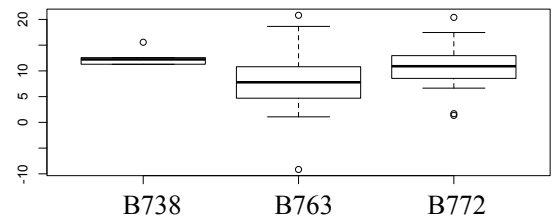
Fig. 3 The Box-plots of the ΔE_i^c

2
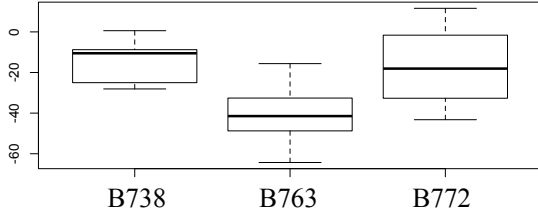
Fig. 4 The Box-plots of the ΔE_i^d

to 3.9%, which meant the range between $(Q3 - Q1)$ was only 3%. For B738, although the data size was extremely small, ΔE also demonstrated a small convergence.

To study the estimation error in detail, three phases (climb, cruise and descent) were defined. TOC (Top Of Climb) and TOD (Top of Descent) were used as the breakpoints of the phases. For each of the phases, the fuel-burn error ΔE_i^b, ΔE_i^c and ΔE_i^d for aircraft i were computed as follows;

$$\Delta E_i^b = (E_i^b - A_i^b)/A_i^b \qquad (2)$$
$$\Delta E_i^c = (E_i^c - A_i^c)/A_i^c \qquad (3)$$
$$\Delta E_i^d = (E_i^d - A_i^d)/A_i^d \qquad (4)$$

where E_i^b, E_i^c and E_i^d were the estimated fuel-burn for each phase and A_i^b, A_i^c and A_i^d were the actual fuel-burn. E_i in (1) is the sum of E_i^b, E_i^c and E_i^d.

Fig. 2, Fig. 3 and Fig. 4 show the box-plots of ΔE^b, ΔE^c and ΔE^d respectively. The median, hinges and whiskers are represented in the same manner as in Fig. 1. From the figures, it was observed that the fuel-burn difference on the descent phase tended to be more spread than the other phases. ΔE^d, particularly for B763, tended to be spread and the medians were much less than zero. To improve the estimation accuracy, the descent phase needs to be focused on.

From the validation results, it was demonstrated that, for the aircraft type B763, the accuracy requires improvements for all the phases. On the other hand, for the other aircraft types, although the accuracy in the descent phase was

deteriorated, the model demonstrated estimation accuracy to some extent.

3 Comparisons of the Efficiency

3.1 Efficiency Measurement

Based on the estimation model, the airborne efficiency is assessed. The efficiency is measured based on the excess fuel-burn from the optimal trajectory.

Knorr et al. measured the flight efficiency as follows[6]. Let F_i be the actual fuel-burn of aircraft i and Opt be the fuel-burn of the optimal trajectory. Flight distance of the optimal trajectory is unimpeded and the optimal trajectory does not contain level-flight before TOC and after TOD.

The excess fuel-burn ΔF_i for aircraft i is represented as

$$\Delta F_i = F_i - Opt \qquad (5)$$

Defining $OptV(d)$ as the fuel-burn function for flight distance d with vertically optimization and d_0 as the unimpeded flight distance, equation(5) can be represented as

$$\Delta F_i = F_i - OptV(d_0) \qquad (6)$$

Furthermore, let d_i be the the actual flight distance of aircraft i. Then, equation (6) can be represented as:

$$\begin{aligned} \Delta F_i = {} & (F_i - OptV(d_i)) \\ & + (OptV(d_i) - OptV(d_0)) \end{aligned} \qquad (7)$$

The first part in equation (7) is the vertical component. It represents excess fuel-burn from the vertically optimized trajectory for the actual flight distance of aircraft i.

The second part is the horizontal component. It represents excess fuel-burn from the unimpeded flight distance.

In this paper, the vertical component is represented as ΔF_{v_i} and the horizontal component is represented as ΔF_{h_i}. As a result, equation (5) can be represented as

$$\Delta F_i = \Delta F_{v_i} + \Delta F_{h_i} \qquad (8)$$

The idea from Knorr et al. described above is used in this study. Since lower excess fuel-burn corresponds to better efficiency, ΔF_v and ΔF_h should be decreased.

3.2 The Computation Method

In this study, trajectory is divided into three areas. The area within a radius of 40 NM of the departure airport is defined as the departure terminal area; the phase within a radius of 100NM of the arrival airport is defined as the arrival terminal area. The area between the two terminal areas is defined as the en-route area.

For the departure and arrival terminal areas, both ΔF_h (horizontal excess fuel-burn) and ΔF_v (vertical excess fuel-burn) are examined. For the en-route areas, ΔF_h is examined.

To compute ΔF_h, actual flight distance d_a is converted into time-amount t_{h_a} as follows.

$$t_{h_a} = \frac{d_a}{v_c} \qquad (9)$$

Here, v_c represents the ground speed on the actual cruise altitude. In equation (7), the trajectories are assumed to be vertically optimized in the horizontal component. Thus, the ground speed of the actual cruise altitude is used. Applying the flight-time t_{h_a} to the BADA table for the cruise altitude, fuel-burn F_{h_a} is obtained.

In the departure and arrival terminal areas, the unimpeded flight distance d_0 is determined based on actual flight distance. For each departure runway, the first quartile is measured and used as d_0. In the same manner, the first quartile of the flight distance in the arrival terminal area is used as d_0 for each arrival runway.

Because radar vectors are used in the destination airport, the standard routes do not play important roles. The shortest flight distance for each departure/arrival runway could be used as d_0. However, since it is not assured that the flight path corresponding to the shortest flight distance

is feasible to all the aircraft, the first quartile is used instead of the shortest distance.

d_0 is converted into time-amount t_{h_s} as follows.

$$t_{h_s} = \frac{d_0}{v_c} \qquad (10)$$

Applying the flight time t_{h_s} to the BADA table for the cruise altitude, fuel-burn F_{h_s} is obtained.

Finally, ΔF_h is computed as follows.

$$\Delta F_h = F_{h_a} - F_{h_s} \qquad (11)$$

Since some of the d_i are shorter than d_0 by definition, ΔF_h might take a negative value. In this case, ΔF_h is regarded as zero value.

In the en-route area, the planned-route distance is applied as d_0. The flight could be vectored to a short-cut course in the en-route area. As a result, ΔF_h takes a negative value. In this case, ΔF_h is regarded as zero value.

For the computation of ΔF_v, the length of actual level-flight segment d_l is measured and it is converted into time-amount t_{v_a} as follows.

$$t_{v_a} = \frac{d_l}{v_a} \qquad (12)$$

Here, v_a is the ground speed on the level-flight segment. For simplicity, the level-flight altitude is assumed to be uniformly 10,000 ft in the departure terminal area and 16,000ft in the arrival terminal area. Applying the flight time t_{v_a} to the BADA table for the assumed altitude, fuel-burn F_{v_a} is obtained.

On the other hand, d_l is converted into another type of time-amount t_{v_c} as follows.

$$t_{v_c} = \frac{d_l}{v_c} \qquad (13)$$

Here, v_c is the ground speed on the actual cruise altitude of each aircraft. Applying t_{v_c} to the BADA table for the cruise altitude, fuel-burn F_{v_c} is obtained. F_{v_c} corresponds to the fuel-burn in which all the level-flight segments are shifted to the cruise altitude.
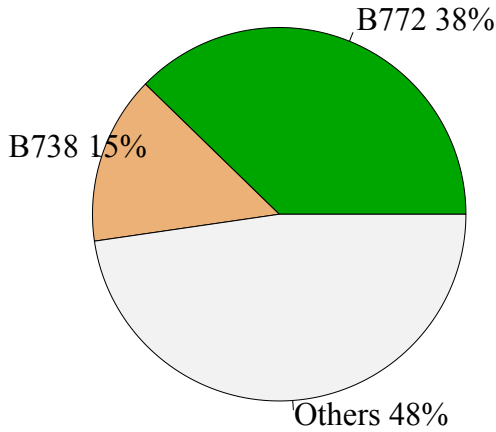
Fig. 5 The Percentages of the Aircraft Types in the Data

Fig. 6 A Comparison of the ΔF

ΔF_v is regarded as the reducible fuel-burn if all the level-flight segments are shifted to the cruise altitude and it is computed as follows.

$$\Delta F_v = F_{v_a} - F_{v_c} \qquad (14)$$

In the computation of ΔF_v, trajectories under the altitude of 5,000 ft in the arrival terminal area are not excluded.

3.3 Data Set

As a principle route in Japanese airspace, the route from Fukuoka (RJFF) to Tokyo (RJTT) was selected and trajectories on this route were analyzed. In this analysis , RDP (Radar Data Processing system) and ARTS (Automated Radar Terminal System) data were obtained and merged.

The ARTS data covered the trajectories within a radius of around 70NM of the destination airport (Tokyo); the RDP data covered the rest of the trajectories. The recording intervals were10 seconds in RDP and 4 seconds in ARTS.

In total, 45 days (13 days in 2007, 6 days in 2009, 6 days in 2010, 20 days in 2011) worth of data were gathered. Based on the validation results in 2.2, the aircraft types of B738 and B772 were selected and 1,112 flights were analyzed . Fig. 5 shows the percentages of the analyzed aircraft type to the total traffic volume on the route.

At Fukuoka Airport, Runway16 and Runway34 were used as the departure runways. Runway 16L, Runway 22, Runway 23, Runway 34L and Runway 34R were used as the arrival runways at Tokyo Airport. For simplicity, Runway 22 and Runway 23 were grouped together as Runway 22; Runway 34L and Runway 34R were grouped together as Runway 34.

In addition, for the estimation of vertical efficiency, level-flight had to be detected from the trajectories. A level-flight segment was defined as more than three consecutive points with an altitude difference of less than 100 feet. In case the points were recorded in ARTS data, the altitude threshold was set to 40 feet instead of the 100 feet to correspond to the different recording time interval.

Table 2 Runway Usage in the Analyzed Data

	Runway	Flight #
Departure	16	822
	34	290
Arrival	16	142
	22	317
	34	653
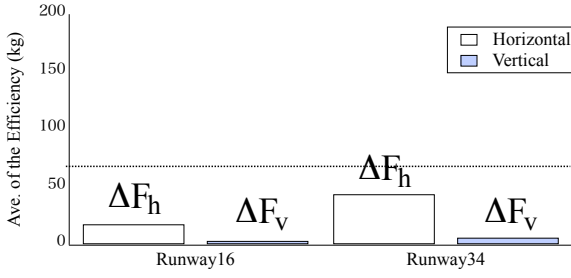
Fig. 7 Comparisons of ΔF in the Departure Terminal Area
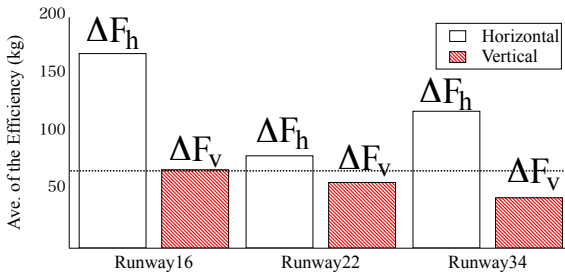
Fig. 8 Comparisons of the ΔF in the Arrival Terminal Area
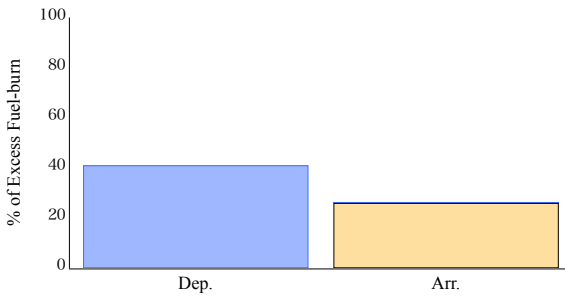
Fig. 9 The Percentages of $\Delta F_v / F_{v_a}$
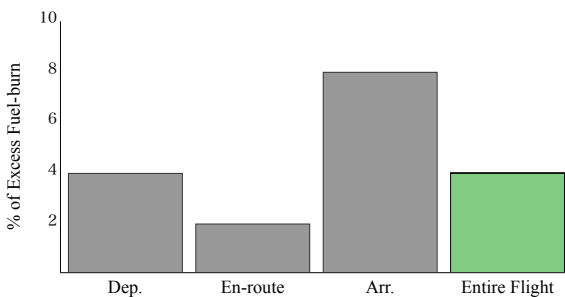
Fig. 10 The Percentages of $\Delta F_h / F_{h_a}$

3.4 Computation Results

Fig. 6 represents a comparison of the averaged excess fuel-burn among the areas. In the chart, the excess fuel-burn in the terminal areas were computed as weighted averages of the departure/arrival runways. It was observed that the excess fuel-burn in the departure terminal area was much lower than the other phases. It was implied that the potential benefit in this area was much less than the others. Also, it was observed that the excess fuel-burn in the arrival terminal area was higher than the others.

In the terminal areas, depending on the runway configurations, the excess fuel-burn could demonstrate different values. Table 2 represents the number of the analyzed flights for each departure/arrival runways. Fig. 7 and Fig. 8 respectively represent comparisons of the ΔF_h and ΔF_v among the runways. The horizontal dotted line represents ΔF_h in the en-route area. It should be noted that the radii of departure and arrival terminal areas were large enough to absorb the effect of flight distance caused by different runway configuration.

In Fig. 7, it was observed that regardless of departure runway configuration, ΔF_v took almost the constant value. At the same time, in Fig. 8, it was observed that, depending on the runway configurations, the ΔF_h varied in the arrival terminal area. In spite of the variation, ΔF_h in the arrival terminal area always exceeded the one in the en-route area.

3.5 Discussion

To investigate the magnitude of the excess fuel-burn, the ratio of ΔF is computed horizontally and vertically.

First, the percentages of vertical excess fuel-burn are shown in Fig. 9. In the figure, the percentage of ΔF_v to F_{v_a} in the departure and arrival terminal areas are shown. The percentages were rather high. It was due to the speed increase accompanying the altitude shift. In the computation of ΔF_h, level-flight altitude was shifted to cruise altitude. As a result, time-amount t_{v_c} and fuel-
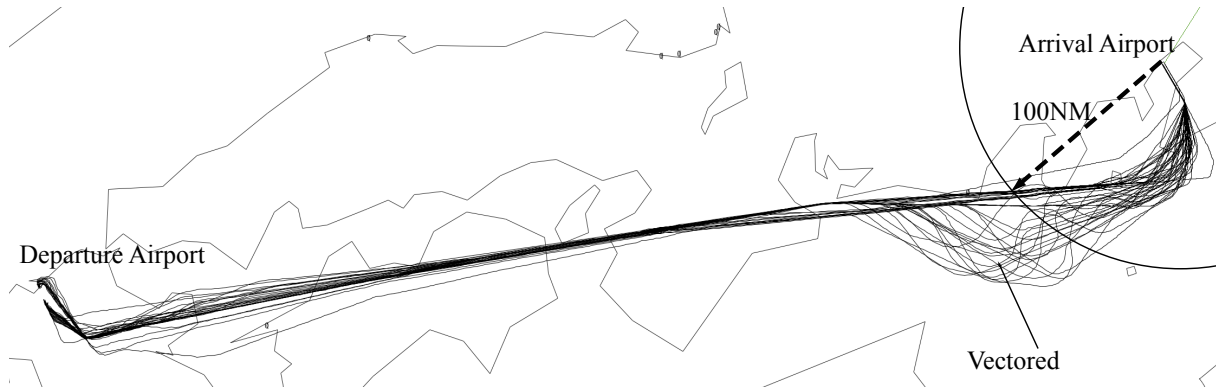
Fig. 11 Examples of the Analyzed Trajectory

burn ΔF_v spent for the level-flight shift was much less than actual values.

It should be noted that although the percentage was high, as shown in Fig. 6, the absolute value of ΔF_v in the departure terminal area was rather small. On the other hand, although the percentage was smaller, the absolute value in the arrival terminal area was much higher than the departure terminal area.

The percentages of horizontal excess fuel-burn are shown in Fig. 10. In the figure, the percentages of ΔF_h to F_{h_a} are compared among the airborne phases. It was observed that the percentage in the arrival terminal area was higher than the others. The percentage in the en-route area was is around 2%, which was a very small number.

In Fig. 10, the percentage for the entire flight is also shown. ΔF_h and F_{h_a} were summed among the areas. The ratio of the sum of ΔF_h to the sum of F_{h_a} was around 4 % for the entire flight.

To investigate the factor of the flight distance stretch in the en-route area, the actual trajectory was examined. Fig. 11 represents examples of the actual trajectory. The circle represents the arrival terminal area. The figure shows that the arrivals were vectored within the arrival terminal area. At the same time, it was observed that the arrivals were vectored outside the circle.

The vectors outside as well as in the arrival terminal area were due to the merging for the destination airport. This figure implies the possibility that the stretch in the en-route area can be

mainly attributed to the arrival merging. In that case, the stretch in the en-route area can be reduced by alleviation of the merging, that is the main factor of horizontal efficiency deterioration in the arrival terminal area.

From the analysis results, it was observed that the potential benefit was mainly deposited in the arrival terminal area.

4 Conclusion

In this paper, basic study of the efficiency in Japanese airspace was shown. First, for the purpose of validation, actual fuel-burn data and estimation results were compared. Except for the aircraft type of B763, the validation results demonstrated accuracy to some extent.

Then, applying the estimation model to actual trajectory of a Japanese representative city pair, fuel-burn was estimated. Based on the estimation results, excess fuel-burn was computed for each of the airborne areas. From the computation results, the arrival terminal area proved to require intensive efficiency improvement. In addition, it was implied that the excess flight distance in the en-route area was mainly attributed to the arrival merging.

It should be emphasized that this study is in the primal stage. To comprehend the airborne efficiency in Japan, it is required to apply the analysis method to the other routes. At the same time, the accuracy of the level flight detection algorithm should be examined. In addition, the def-

inition of unimpeded flight distance needs to be further studied.

Improvements are also required on the fuel-burn estimation model. In particular, because the estimation accuracy proved to be rather deteriorated, estimation for the aircraft type B763 should be intensively examined.

It is without doubt that continuous application of the efficiency study can assist in monitoring and controlling efficiency and consequently offer significant insights into future ATM improvements.

Acknowledgement

The authors are grateful to JCAB (Japan Civil Aviation Bureau), the Ministry of Land, Infr astructure and Transport and Tourism, Japan for their cooperation in the acquisition of the actual performance data. The authors also would like to thank Mr. Kazuo Akinaga for his continuing support and useful advice.

References

[1] SESAR Joint Undertaking. *European Air Traffic Management Master Plan.* 2009.

[2] Federal Aviation Administration. NextGen Implementation Plan. 2011.

[3] International Civil Aviation Organization. *Manual on Global Performance of the Air Navigation System.* 2008.

[4] Performance Review Commission. Performance Review Report 2010. Eurocontrol, 2011.

[5] Project BADA. User Manual for the Base of Aircraft DAta (BADA) revision 3.8. Eurocontrol Experimental Centre,2010.

[6] Marc Rose John Gulding Philippe Enaud Holger Hengendoerfer Dave Knorr, Xing Chen. Estimating ATM Efficiency Pools in the Descent Phase of Flight. In *9th USA/Europe Air Traffic Management Research and Development Seminar*, 2011.

Contact Author Email Address

kage@enri.go.jp

Copyright Statement